

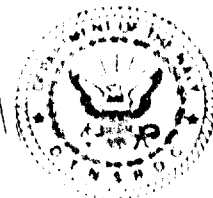
AD A101309

EXPERIMENTAL DEVELOPMENT OF AN ADVANCED CIRCULATION CONTROL WING  
SYSTEM FOR NAVY STOL AIRCRAFT

DTNSRDC-81/045

DAVID W. TAYLOR NAVAL SHIP  
RESEARCH AND DEVELOPMENT CENTER

Bethesda, Maryland 20084



EXPERIMENTAL DEVELOPMENT OF AN ADVANCED  
CIRCULATION CONTROL WING SYSTEM FOR  
NAVY STOL AIRCRAFT

by

J.H. Nichols, Jr.  
R.J. Englar  
M.J. Harris  
G.G. Huson

APPROVED FOR PUBLIC RELEASE: DISTRIBUTION UNLIMITED

REPRINT OF AIAA PAPER 81-0151

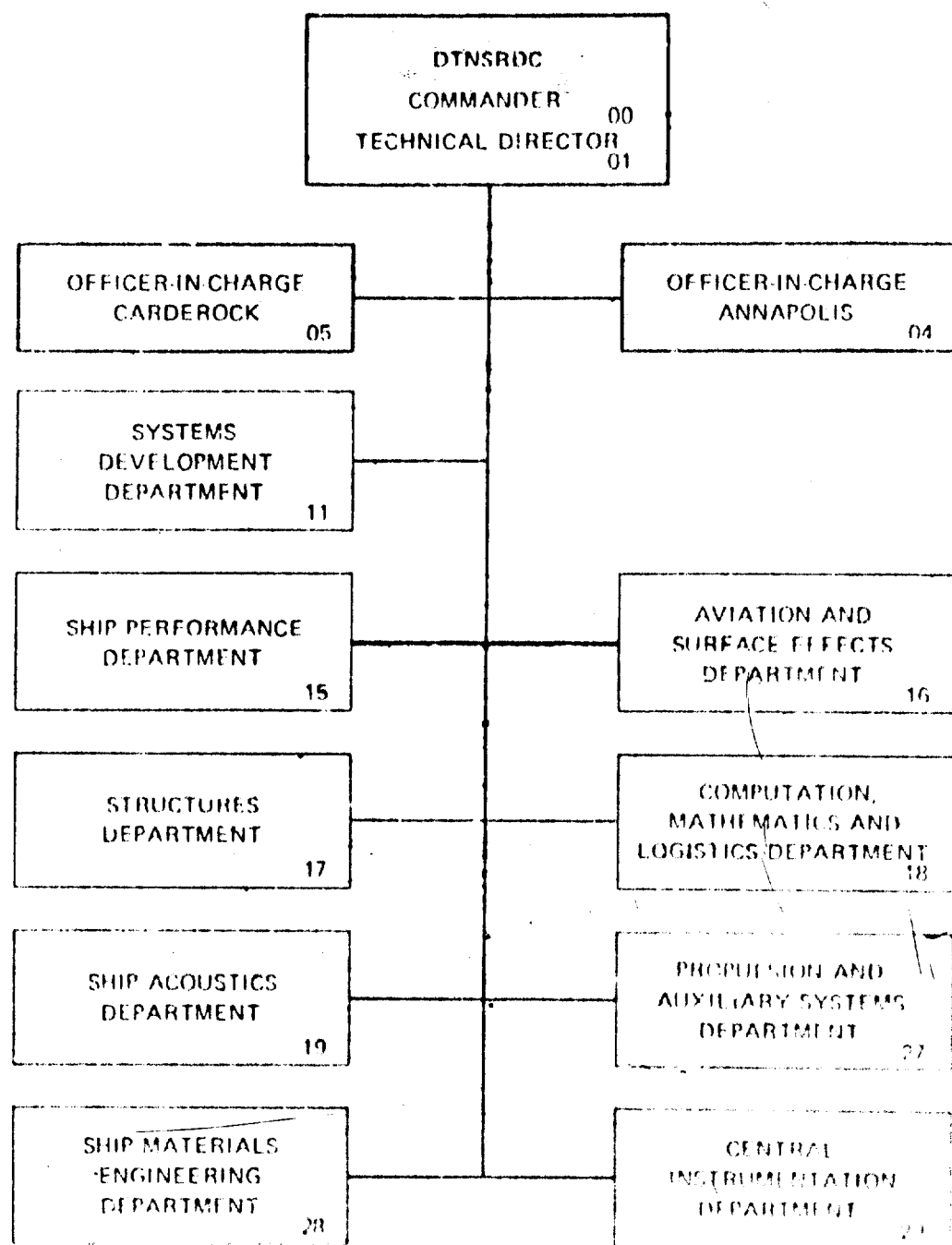
Presented at the AIAA 19th Aerospace Sciences Meeting,  
St. Louis, Missouri,  
12-15 January 1981.

AVIATION AND SURFACE EFFECTS DEPARTMENT  
RESEARCH AND DEVELOPMENT REPORT

May 1981

DTNSRDC-81-045

## MAJOR DTNSRDC ORGANIZATIONAL COMPONENTS



UNCLASSIFIED

SECURITY CLASSIFICATION OF THIS PAGE (When Data Entered)

(9) Research and development  
reptis

REPORT DOCUMENTATION PAGE		READ INSTRUCTIONS BEFORE COMPLETING FORM	
1. REPORT NUMBER <b>(18) DTNSRDC 81/045</b> 2. GOVT ACQ. NO. <b>(19) AD-320 909</b>		3. RECIPIENT'S CATALOG NUMBER <b>TYPE OF REPORT &amp; PERIOD COVERED</b> <b>Acro Report 1272</b> <b>FORMING ORG. REPORT NUMBER</b> <b>(16) P44434</b>	
<b>EXPERIMENTAL DEVELOPMENT OF AN ADVANCED CIRCULATION CONTROL WING SYSTEM FOR NAVY STOL AIRCRAFT.</b>			
7. AUTHOR(s) <b>J.H. Nichols, Jr.</b> <b>G.G. Huson</b> <b>R.J. Englart</b> <b>M.J. Harris</b>		8. ACT OR GRANT NUMBER(s) <b>(16) P44434</b>	
9. PERFORMING ORGANIZATION NAME AND ADDRESS <b>David W. Taylor Naval Ship Research and Development Center</b> <b>Bethesda, Maryland 20084</b>		10. PROGRAM ELEMENT, PROJECT, TASK AREA & WORK UNIT NUMBERS <b>Program Element 62241N</b> <b>(17) Task Area WF 41421 000</b> <b>Work Unit 1600-081-10</b>	
11. CONTROLLING OFFICE NAME AND ADDRESS <b>Naval Air Systems Command (AIR 320D)</b> <b>Washington, D.C. 20361</b>		12. REPORT DATE <b>(11) May 1981</b>	
14. MONITORING AGENCY NAME & ADDRESS (if different from Controlling Office) <b>(14) DTNSRDC/AERO-4272</b>		13. NUMBER OF PAGES <b>17</b> <b>(12) 28</b>	
15. SECURITY CLASS. (of this report) <b>UNCLASSIFIED</b>			
16. DISTRIBUTION STATEMENT (of this Report)  <b>APPROVED FOR PUBLIC RELEASE: DISTRIBUTION UNLIMITED</b>			
17. DISTRIBUTION STATEMENT (of the abstract entered in Block 20, if different from Report)			
18. SUPPLEMENTARY NOTES  <b>Presented at the AIAA 19th Aerospace Sciences Meeting, St. Louis, Missouri, 12-15 January 1981. AIAA Paper 81-0151</b>			
19. KEY WORDS (Continue on reverse side if necessary and identify by block number) <b>Circulation Control/Upper Surface Blowing (CCW/USB)</b> <b>STOL</b> <b>Thrust Turning</b> <b>High Lift</b> <b>Circulation Control Wing (CCW/Supercritical Airfoil)</b> <b>Circulation Control Wing (CCW)</b>			
20. ABSTRACT (Continue on reverse side if necessary and identify by block number)  <b>An advanced high lift system is being developed which combines a Circulation Control Wing (CCW) with Upper Surface Blowing (USB) to produce significant lift for STOL operations by Navy aircraft. The concept uses circulation control to pneumatically deflect USB engine thrust and thus augment aerodynamic wind lift produced by the outboard CCW. Two series of wind tunnel investigations have confirmed significant thrust</b> <b>(Continued on reverse side)</b>			

JL

## UNCLASSIFIED

SECURITY CLASSIFICATION OF THIS PAGE (When Data Entered)

(Block 20 continued)

turning to angles near 160 deg, suggesting the possibility for a simple, highly effective STOL and thrust reverser system. Two-dimensional investigations of reduced diameter CCW trailing edges suggest their application as a no-moving-parts high lift system with minimal cruise penalty. The paper presents these experimental results and summarizes the technology development progressing towards an advanced STOL aircraft..

Accession # or Ref ID	
NTIS GRA&I	<input checked="" type="checkbox"/>
DTIC TAB	<input checked="" type="checkbox"/>
Unclassified	<input type="checkbox"/>
Justification	
Re:	
Distribution/	
Availability Codes	
Avail and/or Dist	Special
H	

UNCLASSIFIED

SECURITY CLASSIFICATION OF THIS PAGE (When Data Entered)

## TABE OF CONTENTS

	Page
LIST OF FIGURES . . . . .	iii
ABSTRACT . . . . .	1
INTRODUCTION . . . . .	1
EXPERIMENTAL INVESTIGATIONS . . . . .	2
CCW + CC/USB MODEL . . . . .	2
STATIC THRUST TURNING RESULTS . . . . .	3
WIND-ON THRUST TURNING RESULTS . . . . .	3
SIMULATED THRUST REVERSER . . . . .	4
CCW/SUPERCRITICAL AIRFOIL . . . . .	5
CONFIGURATION DEVELOPMENT . . . . .	6
STOL PERFORMANCE PREDICTIONS . . . . .	7
SUMMARY AND CONCLUSIONS . . . . .	9
FUTURE PLANS . . . . .	10
REFERENCES . . . . .	10

## LIST OF FIGURES

1 - A-6/CCW Flight Demonstrator Aircraft . . . . .	1
2 - A-6/CCW STOL Performance . . . . .	1
3 - Maximum Lift Coefficients for Typical CCW/USB Aircraft Configurations . . . . .	1
4 - CC/USB Engine Thrust Deflector . . . . .	2
5 - Half-Span CCW + CC/USB Model . . . . .	2
6 - CC/USB Static Thrust Turning . . . . .	3
7 - CC/USB Turning Angle and Thrust Recovery Efficiency . . . . .	3
8 - Effect of Blowing and Thrust Variation on Lift Coefficient . . . . .	4

	Page
9 - Drag Polars . . . . .	4
10 - CCW/USB Simulated Thrust Reverser . . . . .	5
11 - CCW/USB Simulated Thrust Reverser Resultant Force Turning, $\alpha_g = 10$ Degrees . . . . .	5
12 - Configurations for 2-D CCW/Supercritical Airfoil Investigations . . . . .	5
13 - 2-D CCW Airfoil Lift Performance . . . . .	6
14 - 2-D CCW Small Radius Airfoil Lift Performance with Varying Slot Height . . . . .	6
15 - 2-D CCW Airfoil Unblown Performance for Cruise Flight . . . . .	6
16 - Proposed CCW + CC/USB STOL Aircraft . . . . .	7
17 - Proposed CCW + CC/USB STOL Aircraft Planform . . . . .	7
18 - $C_L$ Variation with Aspect Ratio . . . . .	7
19 - High Lift Capability of Conventional S-3A and Proposed CCW + CC/USB Aircraft . . . . .	8
20 - Comparative Lift-Off Velocities, Sea Level Tropical Day . . . . .	8
21 - Comparative Unassisted Takeoff Ground Roll, Sea Level Tropical Day . . . . .	8
22 - Equilibrium Approach Speeds, Sea Level Tropical Day . . . . .	9
23 - Kinetic Energy at Equilibrium Touchdown Speed, Sea Level Tropical Day . . . . .	9

EXPERIMENTAL DEVELOPMENT OF AN  
ADVANCED CIRCULATION CONTROL WING SYSTEM FOR  
NAVY STOL AIRCRAFT

J.H. Nichols, Jr.\*, R.J. Englar,\*\* M.J. Harris,<sup>+</sup> and G.C. Huson<sup>++</sup>  
STOL Aerodynamics Group, Aircraft Division  
David W. Taylor Naval Ship Research and Development Center  
Bethesda, Maryland 20084

Abstract

An advanced high lift system is being developed which combines a Circulation Control Wing (CCW) with Upper Surface Blowing (USB) to produce significant lift for STOL operations by Navy aircraft. The concept uses circulation control to pneumatically deflect USB engine thrust and thus augment aerodynamic wing lift produced by the outboard CCW. Two series of wind tunnel investigations have confirmed significant thrust turning to angles near 160°, suggesting the possibility for a simple, highly effective STOL and thrust reverser system. Two-dimensional investigations of reduced diameter CCW trailing edges suggest their application as a no-moving-parts high lift system with minimal cruise penalty. The paper presents these experimental results and summarizes the technology development progressing towards an advanced STOL aircraft.

Introduction

The Circulation Control Wing (CCW) concept is a mechanically simple high lift system which employs tangential blowing over a rounded trailing edge to yield very high lift augmentation with an expenditure of minimum amounts of jet momentum and mass flow.<sup>1,2</sup> The system has been under development since 1970 at David W. Taylor Naval Ship Research & Development Center (DTNSRDC) where the basic concept was developed, and a configuration for proof-of-concept flight test was designed and experimentally evaluated for application to a Navy/Grumman A-6A aircraft.<sup>3</sup> The A-6 flight demonstrator aircraft was modified to the developed configuration<sup>4</sup> and a flight test was conducted to evaluate the high lift and STOL capabilities of the CCW configuration.<sup>5,6</sup> This A-6/CCW demonstrator aircraft is shown during the flight program in Fig. 1. The rounded CCW trailing edge is visible, as are air supply lines, externally mounted for simplicity, carrying engine bleed air to the CCW. These flight investigations conducted by Grumman confirmed the DTNSRDC wind tunnel predictions that CCW could double aircraft lifting capabilities using only bleed air available from the existing engines. Flight speeds as low as 67 knots were demonstrated even though blown  $C_{L_{MAX}}$  and  $V_{STALL}$  were not achieved due to control power limitations. Test results are published in References 4, 5, and 6. A summary of A-6/CCW STOL performance relative to the conventional A-6A aircraft is given in Fig. 2, illustrating the CCW to be a viable system for providing STOL potential for high performance Navy aircraft.

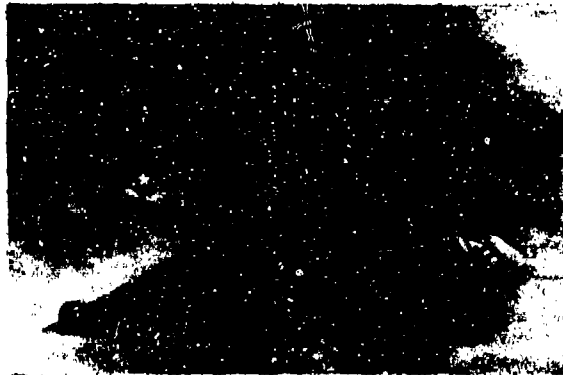


Fig. 1 A-6/CCW Flight Demonstrator Aircraft

BASED ON FLIGHT DEMONSTRATION RESULTS TOOW = 35,700 LB, LGW = 33,000 LB. CORRECTED TO SEA LEVEL, STANDARD DAY		A-6 (30° FLAPS)	A-6/CCW
15% INCREASE IN $C_{L_{MAX}}$		2.1	3.9 ( $C_{\mu} = 0.30$ )
35% REDUCTION IN POWER-ON APPROACH SPEED	118 KTS ( $C_L = 1.40$ )	76 KTS (0.75 $P_{MAX} \cdot C_{\mu} = 0.14, C_L = 2.70$ )	
65% REDUCTION IN LANDING GROUND ROLL	2450 FT	800 FT	
30% REDUCTION IN LIFT OFF SPEED	120 KTS ( $C_L = 1.41$ )	82 KTS (0.8 $P_{MAX} \cdot C_{\mu} = 0.04, C_L = 2.10$ )	
60% REDUCTION IN TAKEOFF GROUND ROLL	1450 FT	600 FT	
75% INCREASE IN PAYLOAD/FUEL AT TYPICAL OPERATING WEIGHT (EW = 28,000 LB.)	45,000 LB.	50,000 LB.	

Fig. 2 A-6/CCW STOL Performance

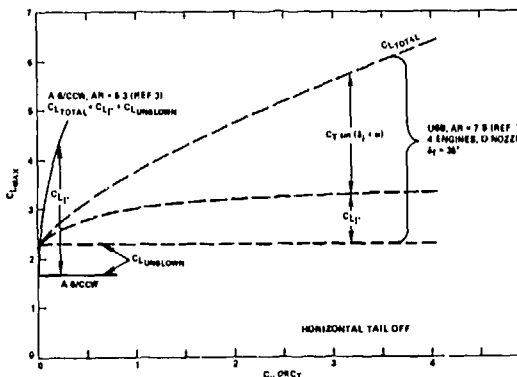


Fig. 3 Maximum Lift Coefficients for  
Typical CCW and USB Aircraft  
Configurations

\*Head, Aircraft Division; Member AIAA.

\*\*CCW Program Manager; Member AIAA.

<sup>+</sup>Aerospace Engineer.

<sup>++</sup>Aerospace Engineer; Member AIAA.

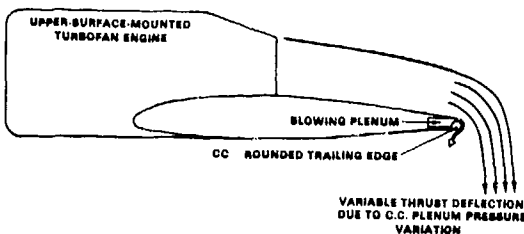


Fig. 4 CC/USB Engine Thrust Deflector

The mechanical simplicity and high lift augmentation of CCW are quite attractive from a weight and STOL performance standpoint. Furthermore, it was envisioned that certain characteristics of the system would be quite compatible with the already proven (YC-14, QSRA, etc.) Upper Surface Blowing (USB) system. Maximum lift coefficients for the A-6/CCW aircraft (aspect ratio 5.3) and a typical 4-engine USB configuration (aspect ratio 7.5) with cruise-typical D-shaped nozzles<sup>7</sup> are shown in Fig. 3. For USB, the incremental lift due to deflecting thrust is made up of the vertical component of the deflected engine thrust,  $C_T \sin(\delta_t + \alpha)$ , with a smaller contribution due to thrust-induced circulation lift,  $C_{L_T}$ . For CCW,<sup>3</sup> the increment of lift due to blowing is all blowing-induced circulation lift,  $C_{L_B}$ , with virtually no vertical thrust component. These large induced lift characteristics logically suggest the physical combination of CCW outboard and USB inboard, to maximize both circulation lift and lift resulting from thrust deflection. Further, by combining Circulation Control (CC) and USB in a CC/USB configuration inboard as shown schematically in Fig. 4, some very significant benefits are obtained by taking advantage of the ability of the circulation control phenomenon to entrain and control the engine thrust direction. The rather complex and heavy USB mechanical flap system and its supporting structure and actuators can be eliminated, and replaced by the stationary CC round trailing edge and internal blowing plenum. For the USB/flap system, thrust deflection angle,  $\theta$ , is achieved by flap upper surface deflection until flow separation occurs. For the CC/USB system,  $\theta$  depends on the CC plenum pressure, slot mass flow, and the flow entrainment effects of the CC trailing edge. That is,  $\theta$  is changed nearly instantly by a flow control valve or pressure regulator. The thrust can be deflected to angles up to 160°, thereby providing a pneumatic thrust reverser, or providing a vertical thrust deflection offering the possibility of VTOL flight. The near-instantaneous thrust deflection variation provides a quick-responding direct lift and flight path control. Initial confirmation of this operation has been reported in Ref. 8.

The keys to achieving the above payoffs are two fold. First is the thrust-deflecting capability of the CC trailing edge, and any limitations placed on that ability by engine thrust levels, nozzle geometry, and freestream dynamic pressure. Second is the CC trailing edge size, which must be small enough for good cruise performance, yet large enough to produce effective supercirculation. To address these items, wind tunnel investigations were conducted to assess STOL performance potential of an aircraft designed around a CCW + CC/USB high lift system.



Fig. 5 Half-Span CCW + CC/USB Model

#### Experimental Investigations

##### CCW + CC/USB Model

The investigation presented herein was intended to evaluate CC/USB thrust-turning capability and made use of an existing generic half-span model that had been used to evaluate CCW and USB systems independently.<sup>9</sup> This model, shown mounted in the DTNSRDC 8- x 10-foot subsonic tunnel in Fig. 5, was a combination of an existing AR = 4 CCW wing section and a USB propulsion simulator. This engine simulator employs two 5.5-inch diameter tip-turbine fans mounted in tandem to generate an output pressure ratio typical of existing turbofan engines, and had previously been used to evaluate low aspect ratio double-slotted flap USB systems employing a variety of exhaust nozzle arrangements. Typical of these nozzles is the D-nozzle shown in the figure, where a simulated internal nozzle flap produced a width/height ratio of 3.3 at the exit.

Independent lift systems were simulated by a series of orifice plates which were inserted in the full-span CCW plenum allowing different duct pressures between the outboard CCW and inboard CC/USB. However, as assembled, the model does not properly represent a typical CC/USB configuration. First, the engine is oversized relative to the wing and is mounted high, resulting in an initial thrust deflection angle of almost 30°. Second, the aspect ratio of 4.0 is lower than that planned for the aircraft/mission to be addressed in this paper.

The airfoil is a 14-percent thick supercritical section with a 15-percent chord Krueger leading edge flap deflected to 40 degrees. CCW trailing edge parameters are based on the A-6/CCW development,<sup>3</sup> viz., a radius-to-chord ratio of 0.036 and a local slot height-to-radius ratio of 0.031. Measured slot height varied nearly linearly with plenum pressure ( $P_{TD}$ ), with a slot area increase of 17 percent occurring at a maximum plenum pressure of 120 in. Hg (58.9 psig). The model was mounted vertically on the tunnel balance frame, independent of a splitter plate and simulated fuselage to remove the wing from the tunnel boundary layer, to simulate fuselage interference, and to allow forces and moments on the wing and engine to be isolated. A thin fence was installed at the wing root to reduce the interaction between any flow from the balance frame and control room and the flow around the wing.

The experiments were conducted in two phases: (1) a static wind tunnel test to quantify thrust turning and select a nozzle, and (2) a wind-on test to quantify thrust turning and thrust reversing during simulated in-flight and landing conditions. Also investigated during the second phase were the effects of higher thrust levels, variations in angle of attack, operation in ground effect, and a configuration build-up to determine individual contributions of CCW and CC/USB.

#### Static Thrust Turning Results

Several exhaust nozzles ranging from round to higher aspect ratio (width/height) D-nozzles were evaluated statically (no freestream) to determine the best nozzle in terms of jet turning. At a constant thrust ( $T$ ) and blowing level ( $\dot{m}V_1$ ), turning ( $\theta$ ) was greatly improved when either the propulsive jet was spread wider and closer to the wing surface, or when the propulsive jet height was reduced relative to the CC slot height. The round nozzles produced relatively little turning because of their large jet height and low aspect ratio of 1.0. The greatest turning performance was provided by the D-nozzle with internal flap shown in Fig. 5. Turning performance of this aspect ratio 3.3 nozzle is shown in Fig. 6, where  $\theta$  is positive for jet turning downward and forward from the aft direction of the chord line, and is determined by resolution of measured horizontal and vertical force components. Resolving the static turning of the CC jet alone with no engine thrust present, shown as the dashed curve, yields  $\theta = 160^\circ$  or more for CC jet plenum pressures greater than 6 psig. (In this figure, static jet momentum/area ( $\dot{m}V_1/S$ ) is equivalent to  $C_u$  at a nominal dynamic pressure of 1 psf). This dashed curve represents an upper limit on propulsive jet turning that could be produced. With the application of engine thrust, several interesting trends are revealed. Increasing CC jet momentum and pressure while maintaining a constant thrust increases the static turning angle. With  $T = 23.3$  lbs the maximum turning achieved is equal to the  $160^\circ$  produced by the CC jet with no thrust present. At higher thrust levels, less turning occurs due to the higher thrust kinetic energy levels which are more difficult to entrain and deflect. However, once  $95^\circ$  of turning was reached at a given thrust level, small changes in CC jet momentum produced rapid increases in turning. Maximum thrust values for a typical turbofan engine

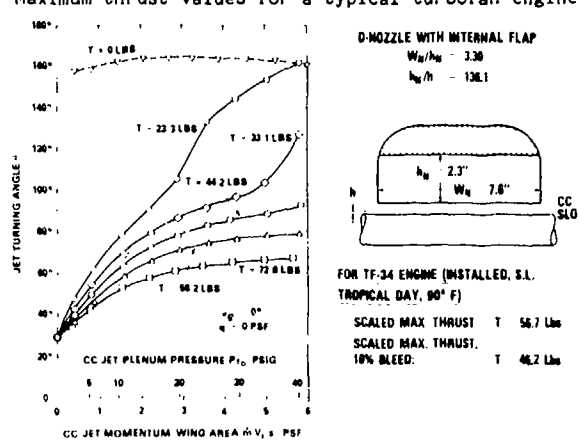


Fig. 6 CC/USB Static Thrust Turning

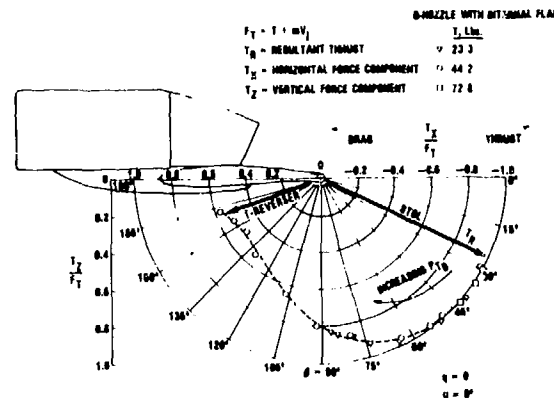


Fig. 7 CC/USB Turning Angle and Thrust Recovery Efficiency

with an exhaust pressure ratio of about 1.5, both with and without core bleed to provide the plenum pressure, are shown for comparison scaled to the model engine. These scaled values are from full scale TF-34 installed thrust for sea level tropical day (90°F) conditions with a 60 knot vehicle speed. A static turning angle of  $80^\circ$  can be achieved at maximum thrust, with values ranging up to  $160^\circ$  at lower thrust levels. This amount of jet turning clearly provides ample thrust deflection for STOL takeoff and approach operation, as well as for reversed thrust upon landing. Also implied here is the possibility of a no-moving-parts VTOL system where static thrust deflection of  $85^\circ$  to  $95^\circ$  can provide vertical lifting and control capability. These thrust turning capabilities and associated thrust recovery are shown in Fig. 7. Here, the denominator  $T_T$  is the sum of the calibrated engine thrust (with no turning) plus the measured momentum of the CC jet, and thus includes all energy input to the system. The length of the vector  $T_R$  represents effective thrust recovery and its direction is the turning angle  $\theta$ . For STOL operation (say  $\theta \leq 60^\circ$ ) more than 95 percent of the input energy is recovered, while as a thrust reverser, 55-60 percent of the thrust is reversed through  $160^\circ$ .

Data similar to the above were also taken in the presence of a fixed groundboard with the wing at zero degrees incidence and heights above the ground plane of 1, 3, and 5 times the mean aerodynamic chord  $\bar{c}$ . For these data with no free-stream, the minimum groundboard height-to-chord ratio of 1.0 produced no significant change in static turning relative to data taken out of ground effect.

#### Wind-on Thrust Turning Results

The degradation of thrust turning due to dynamic pressure ( $q$ ) was measured for flight speeds typical of takeoff and approach. The results are presented in terms of the aerodynamic forces resulting from thrust turning. For this discussion, "drag" ( $C_D$ ) includes the measured horizontal thrust component. The momentum coefficient,  $C_u$ , is defined as nondimensionalized CC jet momentum,  $\dot{m}V_1/S$ . From recent practical experience with engine air availability, a  $C_u = 0.30$  is probably a maximum, yet reasonable value for the near term.

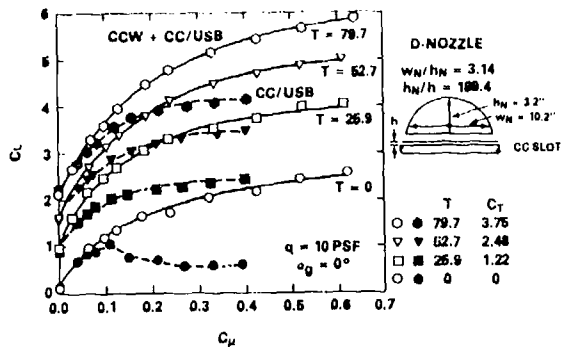


Fig. 8 Effect of Blowing and Thrust Variation on Lift Coefficient

The lift coefficient for constant thrust is presented as a function of  $C_\mu$  in Fig. 8. Corresponding drag polars (including thrust) are presented in Fig. 9. In both figures, the solid symbols and dashed curves represent simulated CC/USB operation, that is, blowing along only that portion of the CC slot immersed in the propulsive jet. The open symbols represent simulated operation of the outboard CCW in addition to the inboard CC/USB. In this latter case, for the data shown both systems are operated at the same slot height and duct pressure. These data were generated at a  $q = 10$  psf (about 55 knots) and a geometric angle of attack ( $\alpha_g$ ) of  $0^\circ$ . For this portion of the test, a D-nozzle design (shown in Fig. 8) more representative of a lower cruise drag shape (and without an internal flap) was used. This nozzle produced static turning results similar to those described in the previous section.

For this CCW + CC/USB operation, 63% of the CC jet momentum operates the inboard CC/USB section and 37% operates the outboard CCW section. At a constant thrust setting, both lift and drag can be increased by increasing  $C_\mu$ . When  $C_\mu$  is held constant (a constant momentum only if  $q$  is not changed), an increase in thrust produces a greater lift; however, the resultant drag is lower due to the contribution of increased thrust.

Selecting a thrust,  $T = 52.7$  ( $C_T = 2.48$ ), nearly representative of the scaled TF-34 turbofan engine, and a  $C_\mu = 0.30$ , more detailed examination of low speed system performance at  $\alpha_g = 0^\circ$  can be made. A maximum  $C_L$  of about 3.4 was produced by operating CC/USB. With a negative drag ( $C_D = -0.4$ ), i.e., a positive thrust. By reducing the thrust to  $T = 25.9$ , and holding  $C_\mu$  constant at 0.30, a  $C_L$  of about 2.3 is produced, but now a positive drag ( $C_D = 0.4$ ) of about the same magnitude as before is available. The addition of blowing to the outboard CCW ( $C_\mu = 0.30$  along the full span) produces a  $C_L = 4.4$  at  $T = 52.7$ , with little change in drag ( $C_D = -0.3$ ). Again, by reducing thrust to  $T = 25.9$ , a  $C_L = 3.5$  still can be produced, but again with a positive drag ( $C_D = 0.5$ ). Thus, even at high lift, aerodynamic drag and thrust (or thrust recovery) can be controlled to produce acceleration or deceleration, or balanced ( $C_D = 0$ ) to allow equilibrium flight. This demonstrates the CCW + CC/USB system's versatility through its ability to produce a large range of high lift with either:

(1) a positive thrust with minimized induced drag

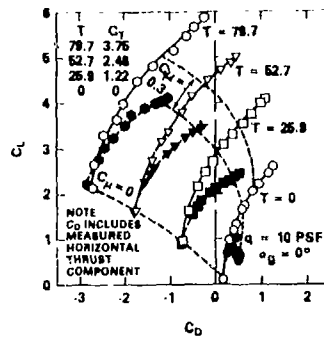


Fig. 9 Drag Polars

for takeoff and climb, (2) a net drag for deceleration upon landing, and (3) a zero net drag for a wide range of flight variables for an equilibrium approach path.

#### Simulated Thrust Reverser

The addition of a simple thrust reverser to a powered lift STOL aircraft can further reduce the already short landing distance provided by low touchdown velocities and reduced kinetic energy. An effective thrust reverser must provide maximum thrust turning, quick response after touchdown, reduction in lift to increase weight on the wheels to improve braking efficiency, and mechanical simplicity. The CCW + CC/USB model was used to simulate landing ground rolls at zero degrees incidence with a fixed groundboard located at  $1.0\delta$  below the model center of gravity. These simulated ground rolls were conducted at constant thrust and plenum pressure by taking data as the tunnel dynamic pressure was reduced by steps from 20 to 0 psf. Therefore, the results indicate the maximum turning possible for the conditions simulated. The data are steady-state and do not give a complete indication of thrust reverser operation during an actual landing. In practice, it may be desirable to turn off the CCW system after touchdown.

Fig. 10 depicts forces generated by a thrust of 24.5 lbs with plenum pressures of 0 and 80 in. Hg. The terms lift and drag here are synonymous with measured vertical and horizontal forces at  $\alpha = 0^\circ$  along the deck, including the corresponding components of thrust. Thus, for blowing off ( $P_{TD} = 0$ ), thrust recovery (or negative drag) increases as the aerodynamic drag decays with dynamic pressure. At zero velocity, almost 90 percent of the initial thrust is recovered as a forward horizontal force, with a vertical component of nearly 50 percent resulting from a downward deflection of about  $30^\circ$  due to the USB nozzle/wing arrangement. With a plenum pressure of 80 in. Hg applied, drag remains positive, directed aft over the entire speed range. The remaining lift at low velocity is about half the value at  $P_{TD} = 0$ , thus providing improved braking force. At zero velocity, these force components with blowing on include approximately 10.2 lbs of drag and 2.7 lbs of lift due to the reaction force of the CCW jet momentum alone. Turning off the outboard CCW plenum would reduce these values by roughly half, resulting in a net drag of 86 percent of the input engine thrust and a lift of only 10 percent of this thrust.

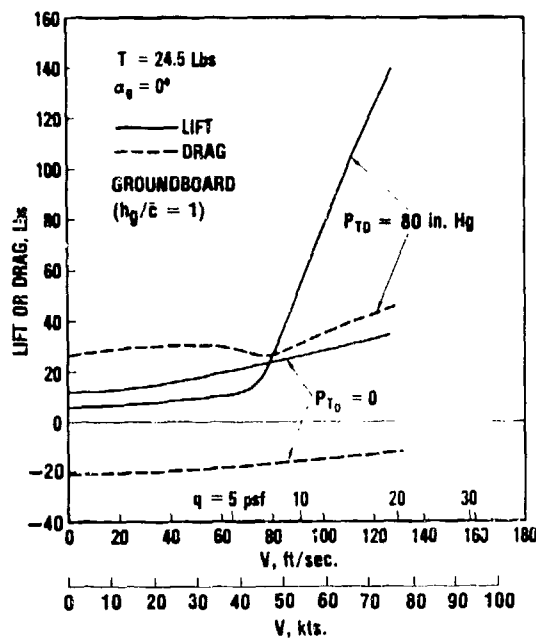


Fig. 10 CCW/USB Simulated Thrust Reverser

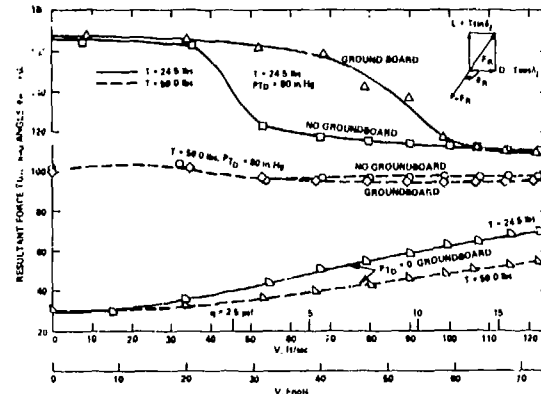


Fig. 11 CCW/USB Simulated Thrust Reverser Resultant Force Turning,  $\alpha_g = 10^\circ$

The resultant force turning angles from the thrust reverser simulation are shown in Fig. 11 for thrust settings of 24.5 and 59.0 lb and blowing pressures of 0 and 80 in. Hg, both with and without a fixed groundboard. Here, the resultant force angle  $\theta_R$  is defined as  $(180^\circ - \arctan(\text{vertical force}/\text{horizontal force}))$ . This angle  $\theta_R$  is similar to  $\theta$  in Fig. 8, except it now includes outboard CCW aerodynamic forces which are not easily separated from inboard thrust components when a freestream is present. At zero velocity,  $\theta = \theta_R$  and the resultant force  $F_R$  equals the sum of the thrust and jet momentum components only. For a thrust of 24.5 lb with blowing in ground effect, force turning rapidly rises from 110° to 165° as speed decreases below the touchdown value of about 55 knots. Without a groundboard, that rise does not occur until speed decreases to about 25-30 knots. An aircraft near touchdown would probably fly on the favorable ground effect curve; speeds of less than 50 knots are not likely prior to the landing ground

roll. For a thrust of 59 lb with blowing, the turning angle is somewhat less than above, but almost constant with decreasing velocity and with much less dependency on ground effect. For no blowing, all thrust levels decay to the configuration's initial angle of 30°. It appears that thrust reversal is quite responsive to both thrust and blowing levels and that a simple no-moving-parts system is feasible.

#### CCW/Supercritical Airfoil

The A-6/CCW design was based on a large radius CC trailing edge surface to guarantee a successful flight demonstration. Any operational use of that particular design would involve some degree of mechanization for conventional flight with a sharp trailing edge. A key to maximizing the effectiveness of the CC high lift/thrust deflecting system is to minimize the impact on cruise performance without requiring mechanization of the CC surfaces. The blunt trailing edge design of a NASA supercritical airfoil can accommodate a small CC trailing edge nearly within the established contour. However, although a physical fit is possible, it is necessary to insure that such an arrangement is still capable of providing effective CC turning for high lift while maintaining the unblown drag at the basic supercritical airfoil level.

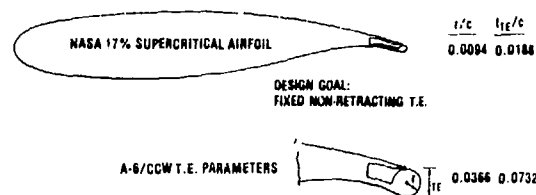


Fig. 12 Configurations for 2-D CCW/Supercritical Airfoil Investigations

A two-dimensional (2-D) wind tunnel investigation was conducted at DTNSRDC to measure the performance of this CCW/supercritical airfoil having a compact 1.9% thick trailing edge (shown in Fig. 12). This supercritical airfoil has a leading edge radius of 4.3% of the chord and normally has a bluff trailing edge thickness of 0.8% of the chord.<sup>10</sup> The larger CC radius trailing edge having 7.3% thickness duplicates the parameters already proven on the A-6/CCW and serves as a state-of-the-art reference. Comparative lifting performance of the supercritical airfoil with both trailing edge geometries is shown in Fig. 13 at  $\alpha_g = 0^\circ$  and  $q = 10$  psf. Also shown in this figure for reference are 2-D data for the A-6/CCW airfoil (7.3% chord trailing edge thickness with a 37.5° leading edge slot). At a likely maximum  $C_L = 0.3$ , the reduction in trailing edge radius yields a loss of 8% of the lift generated by the larger radius at the same slot height. Where leading edge devices were required on the A-6 conventional airfoil, the large bluff leading edge of the 17% supercritical airfoil can avoid flow separation in the region of very high supercirculation during high lift generation ( $C_L$  approaching 8). This is of

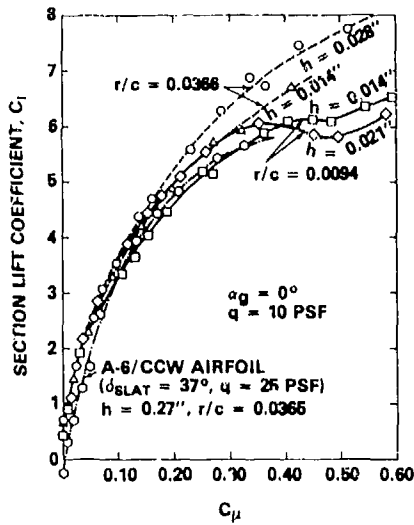


Fig. 13 2-D CCW Airfoil Lift Performance

considerable significance since this potentially further reduces the complexity of a high lift system installation.

The geometry of the small radius trailing edge yields increased values of the important parameter  $h/r$  relative to the large configuration. Variation of lift generated by four different slot heights is shown in Figure 14 as a function of blowing pressure ratio  $P_b/P_\infty$ . Larger slot heights produce higher  $C_l$  and thus higher lift at a given pressure ratio. These larger slot heights also encounter earlier peaking of the lift curve since strong jet attachment becomes more difficult for thicker jets at higher total pressures. However, for airfoil sections powered by turbofan bypass air at a typical pressure ratio of 1.5, it appears that even the larger slot heights will not encounter lift

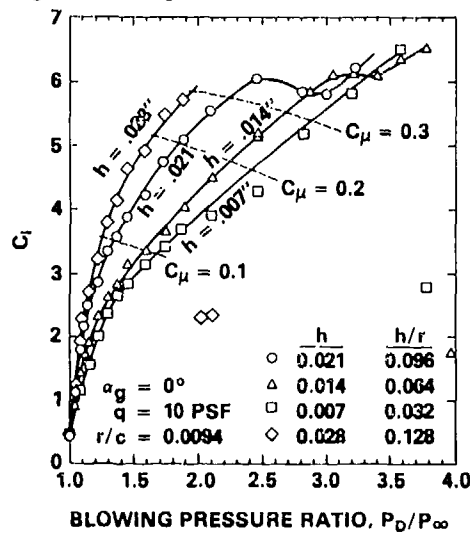


Fig. 14 2-D CCW Small Radius Airfoil Lift Performance With Varying Slot Height

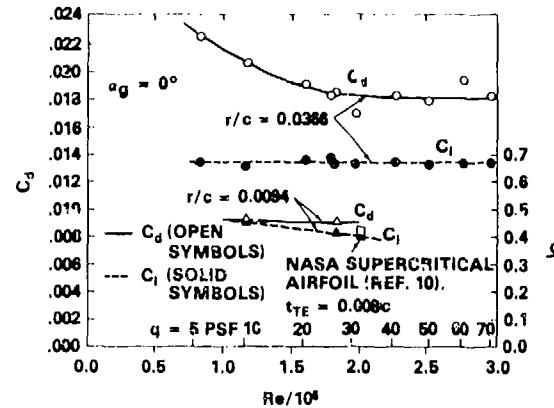


Fig. 15 2-D CCW Airfoil Unblown Performance for Cruise Flight

performance degradation, and are probably more desirable because of the increased  $C_\mu$  available from low supply pressures.

The unblown drag levels of the small radius CCW/supercritical 2-D airfoil are compared to the basic 17 percent supercritical airfoil levels<sup>10</sup> in Fig. 15. At a Reynolds number of 2 million, the drag coefficient of the CCW airfoil is greater than the basic supercritical airfoil by  $\Delta C_d = 0.0006$ . This indicates a minimal drag penalty associated with the small radius CCW airfoil. In addition, the unblown lift appears to be identical to the basic supercritical section. Therefore, the high lift device can remain fixed in cruise flight.

The above data support the small radius configuration as an effective airfoil section possessing the lift augmenting capability of the already proven CCW without the unblown drag penalties, and possibly without a leading edge device.

#### Configuration Development

The above data confirm the feasibility of combining CC/USB with the CCW to produce high lift with a mechanically simple system for a STOL aircraft. The CC/USB no-moving-parts thrust deflection concept can provide a simple light-weight replacement for large mechanical USB/flap systems, and can provide effective thrust reversing with no additional components required. Present USB aircraft like the YC-14 and QSRA combine the inboard USB engine/mechanical flap system with double-slotted mechanical flaps outboard to provide the required lift for takeoff. Replacement of these flaps and outboard drooped or blown ailerons with a CCW trailing edge eliminates the mechanical complexity by allowing transition from the high lift to cruise configuration by terminating blowing. Applied to a relatively thick trailing edge supercritical airfoil, a small-radius CCW trailing edge surface remains fixed at relatively little penalty in cruise drag. A high subsonic STOL aircraft is postulated which employs the CC/USB thrust deflection high lift system inboard and the CCW supercirculation high lift system outboard as shown in Figs. 16 and 17. To provide timely STOL capability without development of a completely new aircraft, the proposed configuration

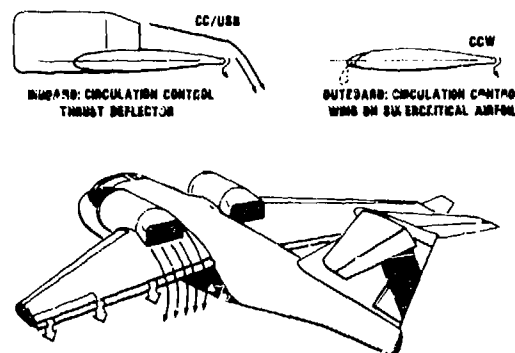


Fig. 16 Proposed CCW + CC/USB STOL Aircraft

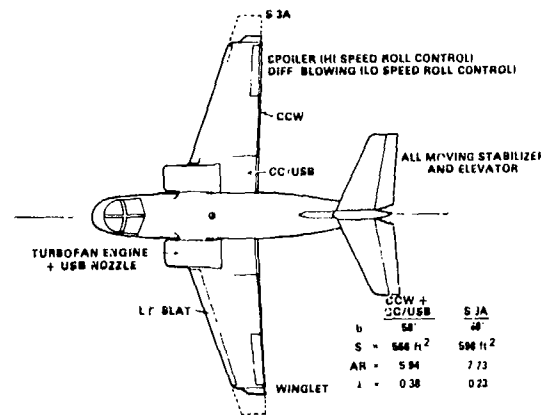


Fig. 17 Proposed CCW + CC/USB STOL Aircraft Planform

makes maximum use of existing Lockheed S-3A aircraft components, namely the airframe, wing primary structure, engines, and as much of the control surfaces as feasible. A supercritical wing with a small radius CCW trailing edge running full span will be installed. The two pylon-mounted TF-34 engines will be moved to the wing upper surface near the fuselage junction. Engine relocation provides the CC/USB thrust turning system, minimizes one-engine-out yawing moments, and reduces air supply crossover line lengths required for controlled flight with one engine out. Two plenums are provided in each wing half. The inboard plenum supplies higher pressure air from TF-34 core bleed for USB thrust deflection. The outboard plenum supplies lower pressure TF-34 fan air to supply the CCW trailing edge. This multi-source air supply system using turbofan core and fan bleed air simultaneously has already been successfully employed on the QSRA aircraft.<sup>11</sup> The inboard and outboard plenums are independently controlled using separate flow valves.

The existing S-3A wing aspect ratio of 7.73 may be retained, or as Fig. 17 shows, removal of 5 ft from each wing tip to reduce the span to 58 ft and AR to about 6 will provide additional flight deck clearance on smaller air-capable ships. The winglets shown may be used to regain effective

aspect ratio in cruise, to carry spanwise high lift distribution closer to the tip, or as directional control devices at low speed. Proposed roll control is by existing spoilers at high speed, and by differential CCW blowing between left and right wings<sup>12</sup> at low speeds. Longitudinal tail location and configuration were not investigated in the present tests. The high T-tail with elevator is shown as being typical of other USB aircraft. However, tail-off pitching moments of the CCW/USB model were similar to those of the A-6/CCW<sup>3</sup> at the same lift coefficient. The A-6/CCW pitching moments were trimmed by a low-mounted all-moving stabilator which benefitted from the additional dynamic pressure and downwash available from the flow field of the engine exhaust. Further investigations are planned to examine longitudinal trim requirements and tail arrangement.

#### STOL Performance Predictions

To predict STOL performance of the proposed CCW+CC/USB aircraft, the existing data must be adjusted to account for the difference in aspect ratio between the model and proposed aircraft. The effect of aspect ratio on  $C_{L_{max}}$  is presented in Fig. 18 for a family of current Navy jet aircraft, for a series of DTNSRDC high lift model data at low aspect ratios of 3 and 4, for existing aircraft with proposed high lift systems, and for several USB configurations. Also shown are two theoretical predictions<sup>13</sup>. The 1.21 AR curve assumes a flat vortex sheet behind the wing. The 1.94 AR curve assumes that the vortex sheet rolls up into two symmetrical vortex cores, which is closer to reality. Neither curve assumes the inclusion of vertical thrust components or thrust-induced lift in  $C_{L_{max}}$ , which explains why several of the USB or CCW/USB data exceed the theory. The trends shown indicate that should the present half-span AR = 4 CC/USB data be extrapolated to AR of 6.0 and 7.7 for the proposed aircraft, the expected  $C_{L_{max}}$  for  $C_T = 2.4$  and  $C_T = 0.33$  is on the order of 8.5 and 10.5, respectively.

To predict estimated lift and drag data for the S-3A-based CCW + CC/USB aircraft within these suggested limits, a more conservative method was

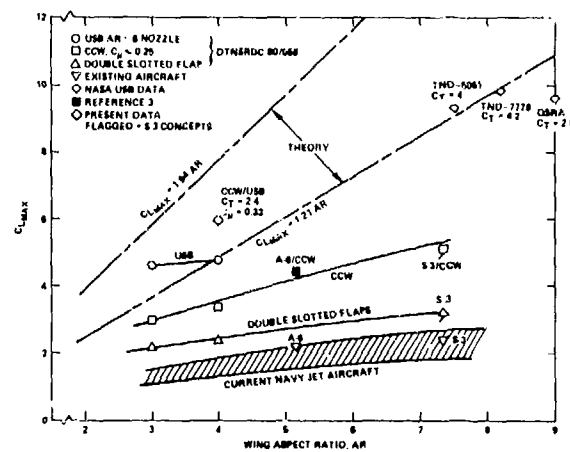


Fig. 18  $C_{L_{max}}$  Variation with Aspect Ratio

used. Fig. 19 shows the resulting lift curves for the AR = 6 configuration. Existing two-engine USB data<sup>14</sup> for incremental lift due to  $C_T$  and jet deflection of 38° were adjusted to the proposed configuration wing geometry. These data were added to lift curves previously developed by Lockheed for an S-3A/CCW configuration using  $C_H = 0.10$  (here labelled  $C_T = 0$ ). A  $C_L^{\text{max}}$  of 6 at  $C_T = 2.4$  and  $C_H = 0.10$  is obtained. These data are conservative since actual thrust deflection angles greater than the 38° assumed can be achieved. The predicted STOL performance shows promising potential even with the conservative data.

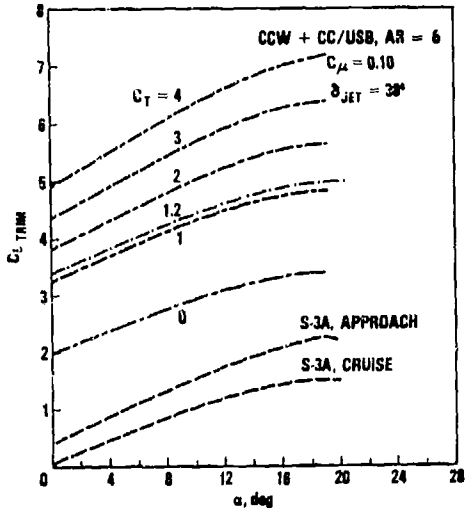


Fig. 19 High Lift Capability of Conventional S-3A and Proposed CCW + CC/USB Aircraft

All STOL performance to be discussed below is based on sea level tropical day (90°F) conditions with standard S-3/TF-34 maximum installed thrust of 13,020 lb total. Losses due to engine thrust droop, bleed, and velocity of 60 knots are included. The proposed AR = 6 configuration is compared in Fig. 20 with the conventional S-3A with AR = 7.73 in terms of lift-off velocity. For a takeoff gross weight range of 35,000 - 40,000 lbs, conventional lift-off speeds of 115 knots can be reduced to 60 - 65 knots. The implications on reduced requirements for catapult equipment (if in fact any is required at all) are significant. The resulting short non-catapulted takeoff distances are compared in Fig. 21 for a wind-over-deck (WOD) velocity of 0 and 20 knots. Here, the takeoff procedure for the proposed aircraft is to accelerate at maximum thrust (bleed off and no thrust deflection) until the rotation speed is reached. At rotation, blowing is initiated and instantaneous thrust deflection and lift augmentation occur. This procedure was successfully and comfortably used by Grumman test pilots with the A-6/CCW<sup>5,6</sup>. Conventional S-3 takeoff rolls of 1,175 - 1,650 ft will be reduced to 200 - 325 ft for a 20 knot WOD. Takeoff distances of 450 - 650 ft are possible if no wind over deck is available. For both conventional and CCW + CC/USB aircraft, the installed thrust-to-weight ratios range from 0.38 - 0.33.

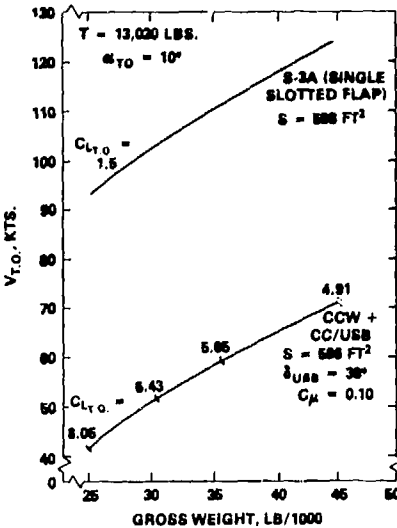


Fig. 20 Comparative Lift-Off Velocities, Sea Level Tropical Day

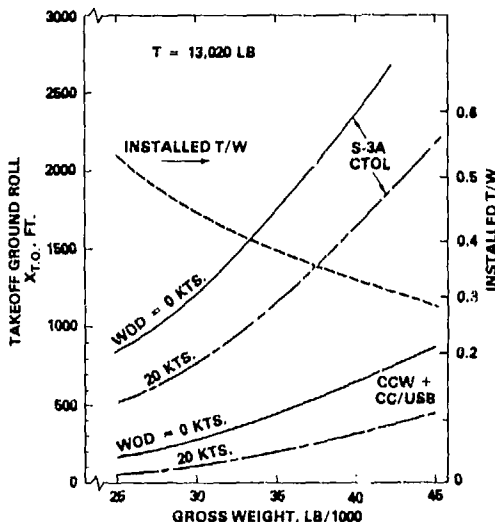


Fig. 21 Comparative Unassisted Takeoff Ground Rolls, Sea Level Tropical Day

Fig. 22 compares equilibrium approach speeds at an incidence of 9° or 10° and on a 4° glide slope. Since no flare is used in Navy approaches, this glide slope is constant and forces must be in equilibrium along that flight path. This requires additional drag generation for USB aircraft since high lift is achieved at high thrust settings which result in high thrust recovery. This thrust recovery is offset for the CCW + CC/USB aircraft by the induced drag generated by CCW. Thus all approaches are made along the  $C_D = 0$  axis of Fig. 9 but at the appropriate approach incidence of 10°. For a landing weight of 30,000 - 35,000 lbs, the approach speed is reduced from 95 to 55 knots by the CCW + CC/USB. For a fixed bleed rate from the

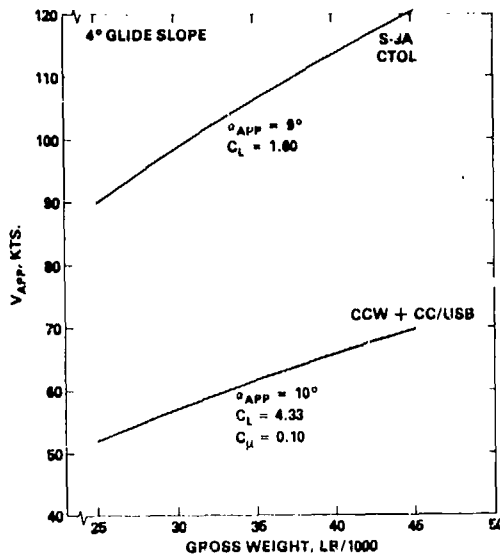


Fig. 22 Equilibrium Approach Speeds, Sea Level Tropical Day

engines, available  $C_{\mu}$  will not remain constant with gross weight as shown Figs. 20 and 22, but will increase as weight decreases. Thus, the actual speeds attainable by the proposed aircraft at lighter weights will be less than those shown if sufficient control power is provided. The reduction in kinetic energy is shown in Fig. 23 at touchdown speeds associated with the above approach conditions. The 70 percent reductions in kinetic energy indicate proportional reductions in landing ground rolls, plus the associated increases in system life. With the proposed CC/USB thrust reverser, there is a strong possibility for reducing or eliminating the arresting gear. These lower approach speeds also imply an improved steeper glide slope to minimize flight through carrier-induced turbulence, increased pilot visibility from approach at lower incidence, and increased pilot reaction time due to lower closure rates, all of which contribute to safer carrier operations and thus reduced accident rates.

The above STOL performance predictions indicate significant potential for aircraft operation from small air-capable ships, plus a number of operational benefits for land-based aircraft as well. They will be refined as additional test data become available and as the proposed aircraft configuration is more adequately defined.

#### Summary and Conclusions

An advanced high lift STOL system combining CC and CC pneumatic USB thrust deflection provides an effective yet simple method to control both wing lift augmentation and the vertical/horizontal force components of the deflected thrust by varying blowing. Experimental results confirm both small trailing edge performance and thrust turning through angles up to 160° plus the associated benefits as a STOL and thrust reverser system, in addition to a potential for VTOL. Application of the test results have led to a proposed conceptual STOL aircraft design to operate from reduced size

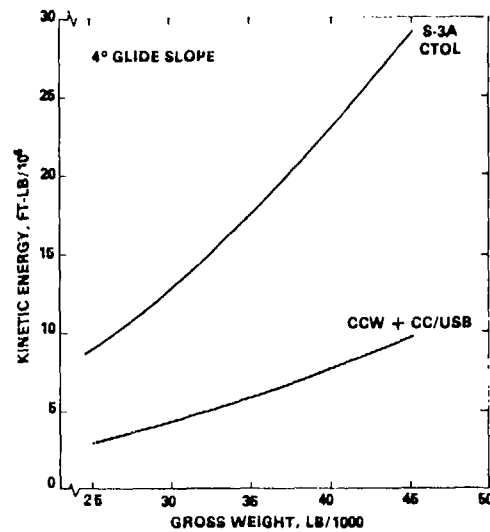


Fig. 23 Kinetic Energy at Equilibrium Touchdown Speed, Sea Level Tropical Day

air-capable ships possibly without the presence of either catapulting or arresting gear.

New capabilities are inherent to this CCW + CC/USB high lift system which are not available in existing or proposed high lift systems. Included in these are:

- Significant improvement in STOL performance is available compared to a conventional flap system (CTOL) on an aircraft with identical weight and thrust; this results from a more than 200 percent increase in maximum trimmed lift coefficient.
- Actuators, flaps, and other high lift system moving parts are reduced by nearly 100 percent.
- High lift, vertical thrust, and thrust reversing can be generated directly from the cruise configuration instantaneously and without external moving parts.
- Direct lift control on approach is independent of thrust setting, and is controlled by changes in the bleed air rate supplied to the wing.
- Higher power setting during approach provides quicker return to maximum thrust for waveoff.
- Low speed lateral control is possible by differential wing blowing.
- A reduced number of parts and reduced impact loads on the aircraft will increase reliability, maintainability and aircraft lifespan.
- Vertical landing and eventually vertical takeoff will be feasible with the above advantages (using thrust deflection in the 90° range) as improved thrust-to-weight powerplants with lower cruise specific fuel consumption become available.

### Future Plans

Whereas the present data base confirms the capabilities of the CCW + CC/USB concept, a considerable amount of additional knowledge about the system is necessary to enable a more detailed design and understanding of the operation of this type of STOL aircraft. The following wind tunnel investigations and design analyses are being planned and will be undertaken to increase the available data base:

- Optimum operation of separate inboard CC/USB and outboard CCW blowing plenums.
- Additional investigations into the effect of freestream dynamic pressure on thrust deflection.
- Determination of longitudinal trim requirements and satisfactory control surfaces.
- Determination of lateral/directional control power requirements and handling qualities.
- Improvement of CC/USB engine nozzles, and effects on cruise performance.
- Determination of cruise configuration performance.

The following tasks are planned to support application of the technology to a test bed aircraft:

- Mission analyses and detailed conceptual aircraft design alternatives with possible alternative engine selection.
- STOL flight simulation using wind tunnel results to investigate handling qualities and develop optimum operation of the blowing/thrust deflection and control systems.
- Construction and static testing of a full size turbofan engine/nozzle/wing CCW + CC/USB configuration to determine scale and temperature effects as well as engine response and core/fan bleed characteristics.

### References

1. Englar, R.J., M.B. Stone and M.Hall, "Circulation Control - An Updated Bibliography of DTNSRDC Research and Selected Outside References," DTNSRDC Report 77-076 (Sep 1977).
2. Englar, R.J., L.A. Trobaugh and R.A. Hemmerly, "STOL Potential of the Circulation Control Wing for High-Performance Aircraft," AIAA Journal of Aircraft, Vol. 15, No. 3, pp. 175-181 (Mar 1978).
3. Englar, R.J., "Development of the A-6/Circulation Control Wing Flight Demonstrator Configuration," DTNSRDC Report ASED-79/01 (Jan 1979).
4. Englar, R.J., R.A. Hemmerly, W.H. Moore, V. Seredinsky, W.G. Valkenaere, and J.A. Jackson, "Design of the Circulation Control Wing STOL Demonstrator Aircraft," AIAA Paper No. 79-1842 presented at the AIAA Aircraft Systems and Technology Meeting, New York (Aug 1979).
5. Pugliese, A.J. and R.J. Englar, "Flight Testing the Circulation Control Wing," AIAA Paper No. 79-1791 presented at AIAA Aircraft Systems and Technology Meeting, New York (Aug 1979).
6. Grumman Aerospace Corporation Report No. FTD-128-55-3.55, "A-6A Circulation Control Wing Flight Test Final Report," (Apr 1979).
7. Sleeman, W.C. and W.C. Hohlweg, "Low-Speed Wind-Tunnel Investigation of a Four-Engine Upper Surface Blowing Model Having a Swept Wing and Rectangular and D-Shaped Exhaust Nozzles," NASA TN D-8061 (Dec 1975).
8. Nichols, J.H., Jr. and R.J. Englar, "Advanced Circulation Control Wing System for Navy STOL Aircraft," AIAA Paper No. 80-1825 presented at the AIAA Aircraft Systems Meeting, Anaheim, California (4-6 Aug 1980).
9. Nichols, J.H. Jr., "Development of High Lift Devices for Application to Advanced Navy Aircraft," DTNSRDC Report 80/058 (Apr 1980).
10. McGhee, R.H. and G.H. Bingham, "Low-Speed Aerodynamic Characteristics of a 17-percent Thick Supercritical Airfoil Section, Including a Comparison Between Wing-Tunnel and Flight Data," NASA TM X-2571 (Jul 1972).
11. McCracken, Robert C., "Quiet Short-Haul Research Aircraft Familiarization Document," NASA Technical Memorandum 81149 (Nov 1979).
12. Englar, R.J., L.A. Trobaugh and R.A. Hemmerly, "Development of the Circulation Control Wing to Provide STOL Potential for High Performance Aircraft," AIAA Paper No. 77-578 presented at the AIAA/NASA Ames V/STOL Conference, Palo Alto, California (6-8 Jun 1977).
13. Whittle, D.C., "Maximum Lift Coefficient for STOL Aircraft: A Critical Review," in Proceedings from CAL/USAAVLABS Symposium on Aerodynamic Problems Associated with V/STOL Aircraft, Vol II, Buffalo, N.Y. (22-24 Jun 1966).
14. Turner, T.R., E.A. Davenport and J.M. Riebe, "Low-Speed Investigation of Blowing from Nacelles Mounted Inboard and on the Upper Surface of an Aspect-Ratio-7.0 35° Swept Wing with Fuselage and Various Tail Arrangements," NASA Memo 5-1-59L (Jun 1959).

INITIAL DISTRIBUTION

Copies	Copies
1 DAR A/LCOL Allburn	15 NAVAIR (Continued)
1 ASN (RE&S) Dr. L. Schmidt	1 AIR 528 1 AIR 5301 1 AIR 5360C4/R. Grosselfinger 1 AIR 6202/J. Madel 1 AIR 950D/Library
1 DDR&E/OSD/R. Siewert	
5 CNO 1 OPNAV 05/VADM McDonald 1 OPNAV 05V/CAPT Cargill 1 OPNAV 506C/CAPT Reach 1 OPNAV 50W1/R. Thompson 1 OPNAV 50W1/CAPT Seibert	1 NISC LT Huska
1 CMC/Sic Advisor A.L. Slafkosky	2 NWC 1 Tech Library 1 Code 3304/P. Amundsen
2 ONR 1 CAPT Howard 1 Code 438/R. Whitehead	2 NAVAIRTESTCEN 1 Dir TPS 1 SA-04C/M. Branch
1 NRL	1 NAVPRO/Bethpage L. Meckler
3 NAVMAT 1 08TC/Dr. Horwath 1 08T22/Remson 1 08TMC/LCO. Bowles	1 DIA P. Scheurich
1 NAVPGSCOL/Library	1 AF Dep Chief of Staff AFRDT-EX
5 NAVAIRDEVCEN 1 Tech Dir 1 Tech Library 1 K. Greene 1 C. Mazza 1 T. Miller	6 AFWAL 1 FDV, STOL Tech Div 1 FDMM, Aeromech Br 2 FIMM 1 Sr. Scientist/Dr. K. Richey 1 AFIT/M. Franke
15 NAVAIR 1 AIR 05 1 AIR 03A/E. Cooper 1 AIR 03E/H. Andrews 1 AIR 03P 1 AIR 03P3 1 AIR 32OD/D. Kirkpatrick 1 AIR 32OF/D. Hutchins 1 AIR PMA 234 1 AIR PMA 244 1 AIR 05	1 AFOSR/Mechanics Div 1 FAA/Code DS-22/V/STOL Program 1 NASA HQ R. Winblade
	6 NASA/AMES Res Cen 1 Tech Library 1 Full-Scale Aero Br 1 Lg-Scale Aero Br 1 QSRA Office/J. Cochrane

Copies	Copies
6 NASA/AMES Res Cen (Continued)	2 General Electric Co
1 B. Lampkin	1 Library
1 A. Faye	1 T. Stirgwort
2 NASA/Dryden	3 General Dynamics/Ft. Worth
1 R. Klein	1 Tech Library
1 T. Ayers	1 W. Foley
6 NASA/Langley Res Cen	1 W. Woodrey
1 Tech Library	1 General Dynamics/San Diego
1 TEPO/J.S. Pyle	Library
1 R. Marguson	
1 J.F. Campbell	1 Georgia Inst of Tech
1 H.D. Garner	Dr. H. McMahan
1 R.W. Barnwell	
1 Analytical Methods	4 Grumman Aerospace Corp
F. Dvorak	1 Library
1 Beech Aircraft Library	1 M. Ciminera
	1 H. Moore
2 Boeing Co/Seattle	1 M. Siegel
1 Tech Library	1 Honeywell, Inc
1 W. Clay	S&R Div
2 Boeing Co/Wichita	2 Hughes Helicopters
1 Library	1 Library
1 L. Frutiger	1 A. Logan
1 Boeing Co/Vertol Div	2 Kaman Aerospace Corp
Tech Lib	1 Tech Library
	1 D. Barnes
1 California Inst Tech	5 Ling-Temco-Vought Inc
P. Lissaman	1 Library
1 Cornell University/Library	1 K. Krall
3 Douglas Aircraft Co	1 J. Louthan
1 Library	1 H. Scherriebl
1 P. McGowan	1 S. Wells
1 F. Posch	
1 Flight Craft Inc	4 Lockheed California Corp
R. Griswold	1 Tech Library
1 Franklin Res Cen	1 J. Hippler
C. Belsterling	1 A. Yackel
	1 H. Yang
	1 Lockheed Georgia Corp
	Library

Copies

2 Northrop Corp/Aircraft Div  
1 Library  
1 W.A. Lusby

1 Pratt & Whitney Aircraft/  
Gov't Products Div  
L. Oglesby

3 Rockwell International/Columbus  
1 Library  
1 P. Bevilaqua  
1 W. Palmer

2 Rockwell International/Los Angeles  
1 Library  
1 M. Robinson

2 Teledyne Ryan Aeronautical  
1 Library  
1 W. Ebner

1 United Tech Corp/E. Hartford  
Library

1 Univ of Maryland/A. Gessow

1 West VA U/Dep Aero Eng  
Library

1 Univ of Kansas/Dr. D. Kohlman

1 Williams Research Corp  
J.T. Wills

CENTER DISTRIBUTION

Copies	Code	Name
10	5211.1	Reports Distribution
1	522.1	Library (C)
1	522.2	Library (A)
2	522.3	Aerodynamics Library